Research Square

Preprints are preliminary reports that have not undergone peer review.
They should not be considered conclusive, used to inform clinical practice,
or referenced by the media as validated information.

Salt tolerance evaluation of seven evergreen Ilex germplasms and transcriptomic insights into photosynthetic inhibition in a sensitive species

Bo Lu
Institute of Botany, Jiangsu Province and Chinese Academy of Sciences
Xinran Chong
Jiangsu Key Laboratory for the Research and Utilization of Plant Resources
Haoran Jia
Jiangsu Key Laboratory for the Research and Utilization of Plant Resources
Chuanyong Wang
Jiangsu Key Laboratory for the Research and Utilization of Plant Resources
Ting Zhou
Institute of Botany, Jiangsu Province and Chinese Academy of Sciences
Bingsong Zheng
State Key Laboratory for Development and Utilization of Forest Food Resources, Zhejiang A&F University
Hong Chen
chenhong@jib.ac.cn

Institute of Botany, Jiangsu Province and Chinese Academy of Sciences

Research Article

Keywords: Ilex genus, Salt stress, Membership function value, Physiological response, Transcriptomics analysis

Posted Date: September 11th, 2026

DOI: https://doi.org/10.21203/rs.3.rs-10651738/v1

License: This work is licensed under a Creative Commons Attribution 4.0 International License.
Read Full License

Additional Declarations: No competing interests reported.

Salt tolerance evaluation of seven evergreen *Ilex* germplasms and transcriptomic insights into photosynthetic inhibition in a sensitive species

Bo Lu[a], Xinran Chong[c], Haoran Jia[c], Chuanyong Wang[c], Ting Zhou[a], Bingsong Zheng[b], Hong Chen[a*]

[a] Institute of Botany, Jiangsu Province and Chinese Academy of Sciences, Nanjing, Jiangsu 210014, China

[b] State Key Laboratory for Development and Utilization of Forest Food Resources, Zhejiang A&F University, Hangzhou, Zhejiang 311300, China

[c] Jiangsu Key Laboratory for the Research and Utilization of Plant Resources, Nanjing, Jiangsu 210014, China

* Corresponding authors

Dr. Hong Chen

Tel: 0086-025-84397121

E-mail: chenhong@jib.ac.cn

Abstract

Global soil salinization calls for the exploration of salt-tolerant plant resources for ecological restoration. *Ilex* species possess both ornamental value and moderate salt tolerance, yet systematic evaluations remain scarce. To address this gap, seven evergreen *Ilex* germplasms were treated with graded NaCl concentrations, and their physiological performance was assessed through photosynthetic parameters, malondialdehyde (MDA), osmoregulatory substances, and chloroplast pigments. Combined with salt injury index (SI), random forest modeling, membership function analysis and transcriptomic sequencing, we comprehensively evaluated salt tolerance and screened core evaluation indicators. It was observed that net photosynthetic rate (Pn), stomatal conductance (Gs), and transpiration rate (Tr) initially increased and then decreased with rising salt concentration. MDA accumulated progressively, while chlorophyll content declined steadily. Osmoregulatory substances exhibited a similar unimodal pattern. Correlation analysis further revealed that SI was positively associated with MDA and proline, but negatively associated with Pn, Tr, and Gs. In addition, random forest analysis indicated that Pn was the primary contributor to salt injury variation (59.3%), followed by Tr (13.6%) and Gs (9.4%), demonstrating photosynthetic capacity as the core indicator for salt tolerance evaluation. Transcriptomic analysis of the most sensitive species, *Ilex dabieshanensis* K. Yao & M. B. Deng, showed that transcriptional regulation gradually shifts from light harvesting to carbon assimilation under salt stress. The pathway “Carbon fixation in photosynthetic organisms” was specifically enriched only under prolonged stress, and Calvin cycle genes exhibited differentiated expression rather than global suppression. Together, these findings present a multi-physiological evaluation framework for salt tolerance in *Ilex*, highlight photosynthetic parameters as promising rapid-assessment indicators, and offer molecular-level

clues regarding photosynthetic inhibition in salt-sensitive germplasm, which may contribute to the breeding and selection of salt-tolerant *Ilex* germplasms for saline-alkali land greening.

Keywords: *Ilex* genus; Salt stress; Membership function value; Physiological response; Transcriptomics analysis

1. Introduction

Global soil salinization is intensifying and causing widespread land degradation, making the identification of salt-tolerant plant resources a key strategy for ecological restoration. According to statistics, more than 6% of the world's land is affected by salinity, covering approximately 831 million hectares, and this area is expanding at an annual rate of 1 to 1.5 million hectares [1]. Salt stress reduces soil water availability, disrupts ionic equilibrium and nutrient acquisition, and induces oxidative imbalance, resulting in a combination of osmotic, ionic, and oxidative stresses that severely affect plant physiological processes and adaptive capacity [2, 3]. Therefore, exploring and utilizing salt-tolerant plant resources is of great significance for the ecological restoration of saline-alkali lands and sustainable greening.

Plants respond to salt stress through coordinated changes in photosynthesis, osmotic regulation, and membrane protection, with photosynthesis being the primary target of salt-induced damage. High salt disrupts chloroplast structure and lowers chlorophyll a (Chl *a*), chlorophyll b (Chl *b*), and carotenoid (Car) contents, impairing light absorption and energy conversion [4]. A close relationship between photosynthetic pigment content and salt tolerance has been established, as salt-tolerant genotypes tend to retain higher pigment concentrations under salinity, thereby supporting more efficient light utilization [5]. In contrast, pigment degradation under salt stress further exacerbates photosynthetic limitation, manifesting as marked declines in net photosynthetic rate (Pn), stomatal conductance (Gs), and transpiration rate (Tr), which collectively reduce carbon fixation and retard growth [6].

Salt stress disrupts not only photosynthesis but also cellular water status and redox balance. To maintain osmotic homeostasis, plants accumulate compatible solutes such as proline, soluble sugars,

and soluble proteins, which reduce osmotic potential and enhance water retention [7, 8]. Meanwhile, salt-induced reactive oxygen species (ROS) overproduction disrupts redox equilibrium and drives membrane lipid peroxidation, with malondialdehyde (MDA) accumulation serving as a sensitive indicator of membrane deterioration [9]. In response, plants bolster their antioxidant systems to mitigate oxidative injury. Among these protective mechanisms, proline stands out as a versatile protectant: it not only contributes to osmotic adjustment but also acts as a non-enzymatic ROS scavenger, participates in redox regulation, and stabilizes proteins and membrane structures under stress [10]. Therefore, photosynthetic performance, osmotic adjustment, and membrane stability are not independent traits but are interlinked through common redox networks that shape the overall plant response to salinity. This interdependence implies that no single physiological index can adequately reflect the full scope of salt tolerance.

ROS accumulation induced by salt stress, while harmful, also initiates cellular stress perception and signaling cascades. Among reactive oxygen species, hydrogen peroxide (H_2O_2) stands out as a particularly effective signaling molecule, owing to its relatively long half-life and ability to cross membranes. Through the activation of antioxidant systems, plants restrict ROS levels to limit oxidative damage while preserving their signaling functions [11, 12]. Beyond their destructive potential, ROS act as secondary messengers that trigger downstream kinase cascades and coordinate adaptive responses. In particular, H_2O_2-mediated mitogen-activated protein kinase (MAPK) cascades have been identified as essential hubs connecting ROS perception to ion regulation and stress signaling [13]. These kinase cascades communicate extensively with phytohormone signaling networks, especially those involving abscisic acid (ABA), to fine-tune stomatal movements, osmotic balance, and the expression of stress-responsive genes [14]. Downstream, diverse

transcription factor families function as key regulatory nodes that coordinate the transcriptional output of salt-responsive genes, forming intricate regulatory webs [15]. Collectively, these signaling and transcriptional events are reflected at the transcriptome level as coordinated changes in genes associated with light harvesting, electron transport, carbon fixation, antioxidant metabolism, and osmotic adjustment [16, 17].

Although salt stress-responsive regulatory networks have been extensively characterized in model plants and major crops, the mechanisms underlying salt tolerance in woody ornamental species remain largely unexplored. As the only extant genus of Aquifoliaceae, *Ilex* comprises more than 400 species worldwide, including approximately 200 species distributed in China, many of which possess significant ornamental and economic value [18]. However, the molecular mechanisms underlying salt stress adaptation in *Ilex* germplasms remain poorly understood. Previous studies have shown that exogenous sucrose can enhance the salt tolerance of English holly (*I. aquifolium*) [19], and transcriptomic analyses have revealed that salt stress responses in *Ilex* involve multiple pathways, including phytohormone signaling, carotenoid biosynthesis, and antioxidant accumulation [20, 21]. However, the existing studies still suffer from notable deficiencies: most investigations have focused on single physiological responses in a limited number of species, lacking a systematic salt tolerance evaluation system; quantitative comparisons of salt tolerance among different germplasms are absent; and the lack of simple and effective evaluation methods makes it difficult to guide the screening of salt-tolerant germplasm and the selection of germplasms for saline-alkali land greening. To address these issues, this study used seven evergreen *Ilex* germplasms as materials, subjected them to different concentrations of NaCl stress, and measured key physiological indicators including photosynthetic parameters,

malondialdehyde, osmoregulatory substances, and chloroplast pigments. By integrating salt injury assessment, random forest modeling, and membership function-based evaluation, we established a comprehensive framework to characterize salt tolerance variation among *Ilex* germplasms and determine the physiological traits most closely associated with salt adaptation. Subsequently, transcriptome sequencing was conducted on the germplasm exhibiting the lowest salt-resilient in the comprehensive assessment to elucidate the underlying molecular responses to salt stress at the transcriptional level. This study provides new insights into the selection of salt-resilient *Ilex* resources, the utilization of superior germplasm for saline-alkali landscape restoration, and the molecular basis of salt stress adaptation in *Ilex*.

2. Materials and methods

2.1. Plant materials

Seven evergreen Ilex germplasms were used in this study, including *Ilex cornuta* Lindl. et Paxt. 'Lutea-carpus', *Ilex*×*cassine*, *Ilex cornuta* 'Dwarf Burfordii', *Ilex* 'Nellie R.Stevens', *Ilex dabieshanensis* K. Yao & M. B. Deng, *Ilex* × 'China Girl', and *Ilex opaca* Aiton. All plant materials were sourced from the same nursery at the Institute of Botany, Jiangsu Province and Chinese Academy of Sciences (118°49′51″E, 32°03′17″N), where they were maintained as rooted cuttings under consistent cultivation practices, including regular watering and quarterly fertilization. To reduce genetic variability, all cuttings were propagated from a single stock plant per germplasm.

2.2. Salt Stress Treatment

Before initiating salt treatment, three-year-old cuttings of each germplasm were established in a greenhouse. The rooted cuttings were individually potted in plastic containers (21.5 cm top

diameter, 19 cm height), and each pot was filled with approximately 5.5 L of a 2:1 (v/v) mixture of nutrient soil and perlite. Rainproof cloths and shade nets were installed in the greenhouse to exclude interference from natural precipitation and excessive light. For each germplasm, seedlings were assigned to six NaCl treatments, with concentrations ranging from 0 to 250 mM at 50 mM increments, each with three replicate groups and five plants per replicate. All seedlings were allowed to acclimatize in the greenhouse for 14 days with regular watering. After the acclimatization period, watering was withheld for 3 days, after which salt stress treatment was initiated. For each pot, 200 mL of the assigned NaCl solution was administered every 3 days; each irrigation was applied slowly until the medium became thoroughly saturated. To prevent salt loss, the leachate collected in trays placed beneath the pots was periodically returned to the pots. Throughout the treatment period, plant growth status and leaf salt injury symptoms were regularly observed, and the progressive severity of symptoms across the NaCl concentration gradient confirmed the establishment of effective salt stress levels. The control group received an equal volume of distilled water following the same irrigation schedule. The treatment lasted for 30 days, during which all other management practices were kept uniform across all treatment groups.

2.3. Photosynthetic Parameter Measurement

Photosynthetic parameters were measured on day 7 of salt treatment. A LI-6800XT portable photosynthesis system (LI-COR) was used for the measurements between 9:00 and 11:00 a.m., according to Zou et al [22]. Fully expanded leaves at positions 3–5 from the apex were sampled from five plants per treatment. Chamber conditions were maintained at 400 μmol mol^{-1} CO_2, 25°C, 1,000 μmol m^{-2} s^{-1} PAR (10% blue/90% red LED), 50% RH, and 500 μmol s^{-1} airflow. Pn, Gs, intercellular CO_2 concentration (Ci), and Tr were recorded.

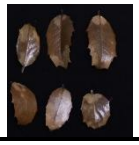
2.4. Salt Injury Index Determination

Salt-induced foliar damage was assessed using the leaf salt injury index (SI) according to the approach described by Yang et al. [23]. The grading system for salt injury levels and the associated visual symptoms of leaves are presented in Table 1. After 30 days of salt treatment, leaf damage was assessed for each germplasm, with 15 plants per germplasm used for statistical analysis. The number of seedlings assigned to each salt injury level was recorded based on the above criteria. Subsequently, SI values were derived from these records to represent the overall severity of salt-induced damage among different germplasms, as described by the equation below.

$$SI = \frac{\sum(SL_i \times N_i)}{N \times SL_{max}} \times 100\%$$

where *SI* is the salt injury index, reflecting the overall severity of salt damage; SL_i is the salt injury level of grade *i*; Ni is the number of plants at grade *i*; N is the total number of plants surveyed; and SL_{max} is the maximum salt injury level value.

Table 1. Grading criteria for salt injury levels and representative phenotypic characteristics under salt stress.

Level	General description	Leaf responses	Plant responses
0	No salt stress injury symptoms		
1	Minor yellowing on leaf tips, margins, and veins; shoots not wilted		
2	Some leaf tips, margins, and veins turn yellow; shoots not wilted		
3	About half of leaf tips and margins scorched; shoots not wilted		
4	Most leaves show tip and margin scorch and defoliation; shoots slightly wilted		
5	Some branches dead, leaves shed, a few plants dead; shoots wilted		
6	Most branches dead, leaves shed, a few plants dead; shoots wilted		
7	All plants dead		

2.5. Physiological and Biochemical Indicator Assays

After 30 days of salt treatment, fresh leaves were collected for physiological and biochemical measurements. MDA and osmolyte contents were quantified following established protocols. MDA was measured using the thiobarbituric acid reaction as described by Hodges et al. [24]. SS, SP, and Pro were determined by colorimetric assays using anthrone [25], Coomassie Brilliant Blue G-250 [26], and ninhydrin [27], respectively. Chl *a*, Chl *b*, and Car were extracted and measured following

[28]. All pigment contents were calculated based on absorbance measurements at the corresponding wavelengths.

2.6. Transcriptomic Analysis of I. dabieshanensis under Salt Stress

To elucidate the molecular mechanisms underlying photosynthetic inhibition in salt-sensitive germplasm, we selected *I. dabieshanensis* for transcriptomic analysis, as this species was identified as the most salt-sensitive through physiological screening (see Section 3.2). The plant materials were derived from the same batch of mother plants as those used in the physiological experiments. Uniform current-year shoots bearing approximately 10 leaves were maintained under controlled growth conditions (22 °C; 16 h photoperiod followed by 8 h darkness) for 14 days before exposure to 200 mM NaCl solution. Samples were obtained at 0, 3, 6, 9, 12, and 24 h after salt application. The third and fourth fully expanded leaves below the shoot apex were collected from six plants and pooled at each sampling point.

The transcriptomic data were derived from our earlier study [21]. To investigate the transcriptional dynamics of photosynthesis-related pathways, we re-analyzed the raw RNA-seq data. The analysis followed the pipeline described previously. A key difference was the use of DESeq2 (v1.42.1) for DEG identification ($|\log_2(\text{fold change})| \geq 1$, FDR ≤ 0.05).In brief, raw reads were trimmed with fastp (v0.24.1) [29], aligned to the *I. paraguariensis* reference genome (ILEXP v3) using HISAT2 (v2.2.1) [30], and quantified as FPKM using featureCounts (v2.0.6) [31]. GO and KEGG enrichment analyses were performed using EggNOG-mapper (v2.0.1) [32] and KOBAS (v3.0) [33], respectively. Enrichment analysis and visualization were conducted in R (v4.4.0) with clusterProfiler [34] and pheatmap (v1.0.12).

2.7. Statistical analyses

The fuzzy membership function method [35] was used to quantitatively transform the eight physiological indicators measured for the seven evergreen *Ilex* germplasms. For each germplasm, the mean membership degree of all indicators was computed. The salt tolerance ranking of the tested germplasms was then assigned according to these mean values using the following formulas.

For variables exhibiting positive relationships with salt tolerance:

$$R(X) = (Xi - Xmin) / (Xmax - Xmin)$$

For variables exhibiting inverse relationships with salt tolerance:

$$R(X) = 1 - (Xi - Xmin) / (Xmax - Xmin)$$

Here, R(X) is the membership degree of a germplasm for a given indicator ($0 < R(X) < 1$), where Xi is its measured value, and Xmax and Xmin are the extreme values among all germplasms. Membership values were computed from the 250 mM NaCl dataset and averaged per germplasm; higher mean values indicate greater salt tolerance.

Statistical analyses were performed using SPSS 27.0 (IBM Corp.), and figures were generated using GraphPad Prism 9.0 (GraphPad Software). Data collected from three biological replicates were subjected to one-way ANOVA, and Duncan's multiple range test was used for post-hoc comparisons at $p < 0.05$. We performed random forest analysis in Python 3.6 (Python Software Foundation) following Li et al. [36]. Data were normalized (min-max scaling) and then split 70/30 into training and testing sets, maintaining representation of all germplasms and treatments across both. Ten-fold cross-validation was used for training, and parameters are given in Supplementary Tables S1.

3. Result

3.1 Physiological responses of seven Ilex germplasms to salt stress

3.1.1 Photosynthetic parameters

At low salt concentrations (0–50 mM), most germplasms showed an increase in Pn. In *I. opaca*, *I. dabieshanensis*, I. *cornuta* 'Dwarf Burfordii', *I.* × 'China Girl', and 'Luteacarpus', Pn at 50 mM NaCl increased by 3.2% to 8.7% compared with the 0 mM control, with *I. opaca* showing the largest increase. In contrast, *I.* × *cassine* exhibited inhibition of Pn at 50 mM, while *I.* 'Nellie R. Stevens' remained stable. At 100–150 mM NaCl, Pn showed a gradual decline in all germplasms, with even greater reductions at 200–250 mM relative to the control (Table 2a).

Table 2a. Variations in net photosynthetic rate of seven *Ilex* germplasms under salt stress

Breed	NaCl concentration					
	0mM	50mM	100mM	150mM	200mM	250mM
I. 'Nellie R.Stevens'	8.745±0.160 a	8.017±0.260 a	6.213±0.180 b	5.693±0.268 b	4.507±0.700c	4.150±0.442 c
I. opaca	6.845±0.327 ab	7.699±0.690 a	6.572±0.202 b	5.093±0.666 c	3.461±0.395d	3.365±0.302 d
I. dabieshanensis	6.885±0.530 a	7.654±0.560 a	5.768±0.859 b	4.993±0.662 b	2.468±0.229c	0.946±0.216 d
I. cornuta 'Dwarf Burfordii'	6.573±0.409 b	8.043±0.395 a	4.723±0.514 c	3.865±0.377 cd	3.130±0.339d	1.364±0.766 e
I. × 'China Girl'	6.324±0.390 a	6.650±0.459 a	5.959±0.558 a	4.508±0.332 b	2.413±0.604c	1.865±0.534 c
I. cornuta Lindl. et Paxt. 'Luteacarpus'	6.939±0.659 ab	7.5412±0.452 a	6.463±0.479 b	3.547±0.273 c	2.202±0.550d	1.061±0.440 e
I.×cassine	6.004±0.399 a	5.082±0.297 a	3.539±0.345 b	1.961±0.558 cd	2.618±0.282 bc	1.134±0.498 d

Note: Means ± SD are presented. Different letters within a germplasm denote significant differences among NaCl concentrations ($P < 0.05$). Subsequent tables follow the same notation.

Gs, Ci, and Tr also exhibited significant interspecific differences in response to salt stress. For stomatal conductance, *I.* 'Nellie R. Stevens' reached its peak value of 0.264 $mol \cdot m^{-2} \cdot s^{-1}$ at 100 mM (61.0% higher than the control) and maintained a value of 0.111 at 250 mM; *I.* × *cassine* had its highest conductance at 100 mM, which dropped sharply to 0.048 at 250 mM; *I. opaca* reached its peak of 0.253 at 50 mM (**Table 2b**).

Table 2b. Variations in stomatal conductance among seven *Ilex* germplasms under salt stress

Breed	NaCl concentration					
	0mM	50mM	100mM	150mM	200mM	250mM
I. 'Nellie R.Stevens'	0.164±0.001ab	0.202±0.034ab	0.264±0.028a	0.187±0.023ab	0.237±0.126a	0.111±0.032b
I. opaca	0.196±0.054a	0.253±0.064a	0.249±0.016a	0.205±0.113a	0.203±0.016a	0.170±0.093a
I. dabieshanensis	0.128±0.040a	0.216±0.052a	0.220±0.098a	0.207±0.003a	0.120±0.020a	0.123±0.001a
I. cornuta 'Dwarf Burfordii'	0.156±0.021ab	0.176±0.012ab	0.225±0.089a	0.210±0.082ab	0.122±0.044ab	0.104±0.030b
I. × 'China Girl'	0.231±0.049ab	0.256±0.004a	0.182±0.040abc	0.128±0.023b	0.108±0.057c	0.079±0.050c
I. cornuta Lindl. et Paxt. 'Luteacarpus'	0.195±0.036b	0.357±0.057a	0.327±0.050a	0.160±0.009b	0.097±0.045 b	0.080±0.028b
I.×cassine	0.152±0.019bc	0.158±0.155abc	0.272±0.107a	0.180±0.064ab	0.127±0.028bc	0.048±0.029c

Ci varied among germplasms: *I. opaca* maintained relatively high and stable Ci across all salt concentrations. In *I.* × 'China Girl', Ci fell steadily with increasing salinity and was significantly lower at high concentrations (150–250 mM) than at low concentrations. In *I.* 'Nellie R. Stevens', *I. cornuta* Lindl. et Paxt. 'Luteacarpus', I. *cornuta* 'Dwarf Burfordii', and *I. dabieshanensis*, Ci showed an initial increase followed by a reduction as salt concentration rose (**Table 2c**).

Table 2c. Changes in intercellular CO_2 concentration of seven *Ilex* germplasms under salt stress

Breed	NaCl concentration					
	0mM	50mM	100mM	150mM	200mM	250mM
I. 'Nellie R.Stevens'	314.129±9.484a	315.521±28.689a	350.491±30.796a	334.676±2.762a	315.443±6.349a	315.305±14.246 a
I. opaca	327.515±5.236a	321.879±11.720a	330.05±28.058a	328.371±10.833a	369.046±6.185a	346.319±22.229 a
I. dabieshanensis	297.267±7.924b	341.653±9.673ab	376.008±5.558a	339.723±17.327ab	309.721±9.553ab	297.03±51.083b
I. cornuta 'Dwarf Burfordii'	306.22±32.268bc	350.392±15.971ab	373.882±13.731a	318.590±18.818bc	315.690±17.275bc	293.034±19.510 c
I. × 'China Girl'	355.201±10.487a	352.815±5.323ab	339.38±23.412ab	314.639±28.475ab	301.899±3.984b	336.110±30.411ab
I. cornuta Lindl. et Paxt. 'Luteacarpus'	324.516±12.881b	320.191±18.974b	380.766±3.022a	362.615±7.338ab	353.085±6.782ab	255.88±64.782c
I.×cassine	320.706±5.517bc	281.809±83.455c	364.730±8.031ab	360.538±18.600ab	374.147±6.087a	343.642±48.957ab

For Tr, most germplasms exhibited an initial increase followed by stabilization at low salt concentrations (0–100 mM), with *I. opaca* showing the highest value at 100 mM, while *I.* × *cassine* and *I. dabieshanensis* also showed relatively high values at 50–100 mM. At high salt concentrations, Tr decreased significantly in most germplasms; at 250 mM, *I.* × *cassine* and *I.* × 'China Girl' showed the lowest values, while *I. opaca* remained relatively high (**Table 2d**).

Table 2d. Changes in transpiration rate of seven *Ilex* germplasms under salt stress

Breed	NaCl concentration					
	0mM	50mM	100mM	150mM	200mM	250mM
I. 'Nellie R.Stevens'	3.470±0.801 ab	3.808±1.662 a	4.866±0.049 a	4.855±0.131 a	4.103±0.094 a	1.934±1.476 b
I. opaca	3.749±1.794 bc	5.783±2.693 a	5.389±0.750 a	4.312±1.378 ab	4.222±0.442ab	2.286±0.823 c
I. dabieshanensis	2.164±1.014 b	4.291±0.858 a	4.091±0.090 a	3.598±0.716 ab	2.473±0.716 b	2.352±0.346 b
I. cornuta 'Dwarf Burfordii'	2.967±1.128 bcd	3.700±0.900 abc	4.550±1.749 ab	4.823±1.605 a	2.491±0.184 cd	1.961±0.355 d
I. × 'China Girl'	3.879± 0.956 ab	4.949±1.768 a	4.132±1.210 ab	3.652±0.853 ab	2.697±0.594 b	0.920±0.383 c
I. cornuta Lindl. et Paxt. 'Luteacarpus'	3.532±1.121 a	3.855±0.626 a	4.638±1.589 a	4.606±1.150 a	4.145±0.326 a	1.765±0.503 b
I.×cassine	2.954±0.598 a	4.382±0.570 a	4.458±0.417 a	3.521±1.125 a	1.108±0.936 b	1.003±1.103 b

3.1.2 MDA content

Across the seven Ilex germplasms, leaf MDA content rose steadily as NaCl concentration increased. *I. dabieshanensis* showed the greatest elevation, with MDA levels increasing by 37.37% relative to the control and peaking at 17.604 μmol·g⁻¹. MDA contents in *I. cornuta* 'Dwarf Burfordii', *I.* × *cassine*, and *I. opaca* were relatively low. In *I. cornuta* 'Dwarf Burfordii' and *I.* × *cassine*, MDA content increased in a stepwise manner from 0 to 200 mM NaCl and showed a sharp rise at 250 mM. In 'Luteacarpus' and *I.* 'Nellie R. Stevens', MDA content increased only slightly under low and moderate salinity, but rose markedly at 200 mM and 250 mM. In *I.* × 'China Girl', MDA content gradually increased with increasing salt concentration, with the maximum value being 71.18% higher than the control. In *I. opaca*, MDA content was significantly higher than the control across the 50–150 mM range, with no significant differences among these concentrations, but showed a substantial increase at 200 mM (**Fig. 1**).

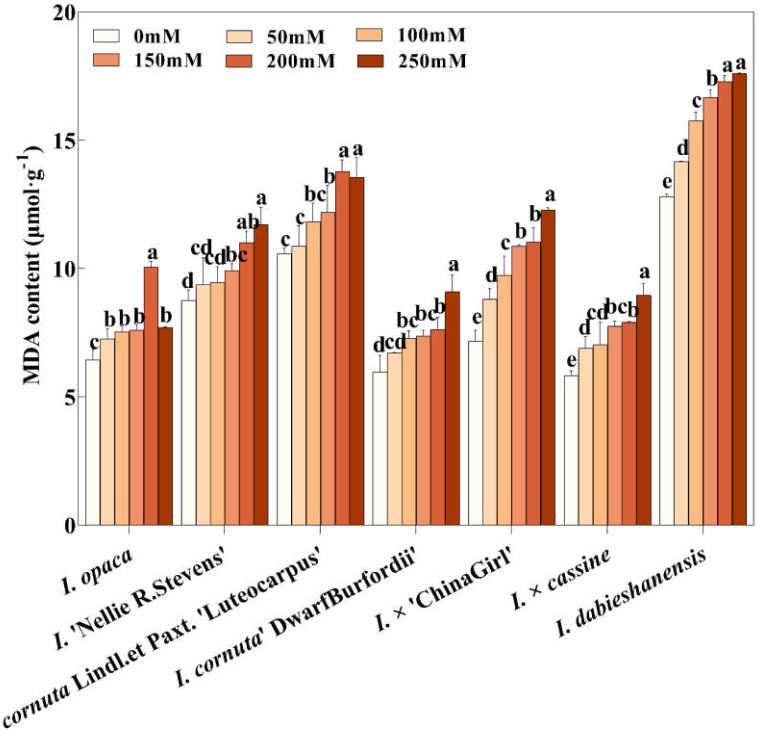


Fig. 1. Leaf MDA content of seven Ilex germplasms under salt stress. Error bars represent SD (n = 3). Different lowercase letters denote significant differences among salt concentrations in each germplasm ($P < 0.05$), and the same applies to Figures 2–4. MDA, malondialdehyde. Abbreviations are consistent across all tables and figures.

3.1.3 Osmotic regulatory substances

With increasing NaCl concentration, SS, SP, and Pro contents in the seven *Ilex* germplasms changed dynamically, first rising and then falling. For SS, most germplasms reached their maximum values at moderate to high concentrations (100–200 mM), followed by a significant decrease at 250 mM, with interspecific differences observed: *I. opaca* peaked at 100 mM with an increase of 28.18% over the control; *I.* × 'China Girl' showed an anomalous increase only at 100 mM; 'Luteacarpus' increased by 24.97% at 150 mM compared with the control, with a decrease of 4.75% at 250 mM; both *I. dabieshanensis* and *I. cornuta* 'Dwarf Burfordii' reached their highest values at 200 mM (**Fig. 2A**). SP content exhibited species-specific responses: both *I.* 'Nellie R. Stevens' and 'Luteacarpus' reached their maximum values at 150 mM, with increases of 25.83% and 27.79%, respectively, over the control; *I. cornuta* 'Dwarf Burfordii' peaked at 200 mM, reaching 17.874

277 mg·g^{-1} (a 70.80% increase); at 250 mM, SP content declined significantly in all germplasms (**Fig.**
278 **2B**). For Pro, *I.* × ‘China Girl’ reached its highest value at 150 mM (a 65.70% increase over the
279 control), which was the highest among all germplasms; ‘Luteacarpus’ reached 176.417 μg·g^{-1} at
280 150 mM (a 10.81% increase), significantly lower than in other germplasms; *I.* ‘Nellie R. Stevens’
281 decreased by 8.35% at 250 mM compared with 100 mM; *I.* × *cassine* peaked at 50 mM (248.224
282 μg·g^{-1}) and then declined continuously; *I. dabieshanensis* decreased by 25.64% at 250 mM
283 compared with 100 mM; *I. cornuta* ‘Dwarf Burfordii’ and *I. opaca* reached their maximum values
284 at 150 mM, with decreases of 24.64% and 17.97%, respectively, at 250 mM; notably, Pro content
285 in *I. opaca* showed no significant differences among treatments (**Fig. 2C**).

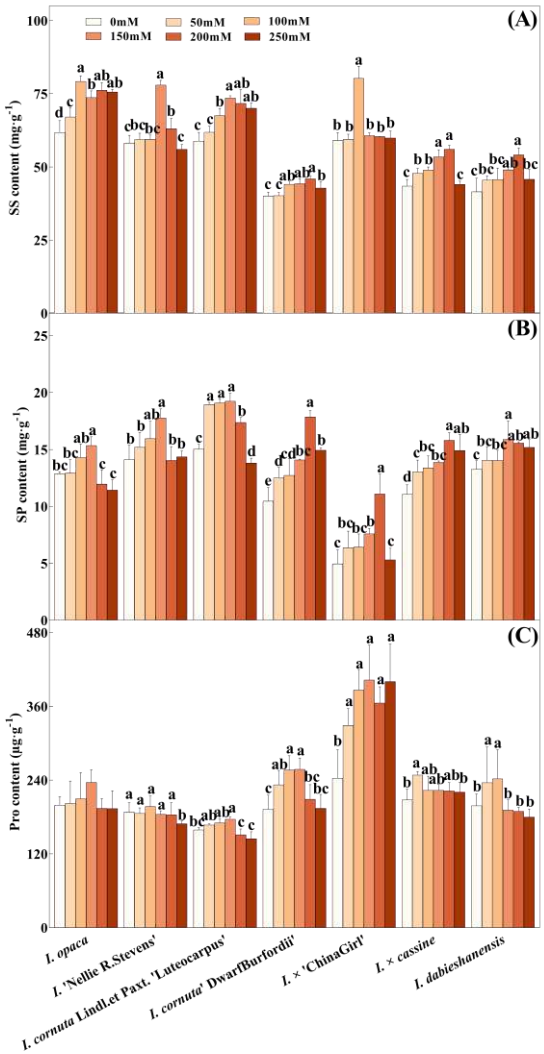


Fig. 2. Changes in Osmotic regulatory substances in seven *Ilex* germplasms under salt stress. SS, soluble sugar; SP, soluble protein; Pro, proline. Same abbreviations apply to all tables and figures below.

3.1.4 Chloroplast pigment content

Among the seven Ilex germplasms, six showed a unimodal response in chloroplast pigment content to increasing NaCl concentration (0–250 mM), first rising and then falling. In contrast, *I. dabieshanensis* displayed no obvious trend, with pigment content consistently lower than the control. In *I.* 'Nellie R. Stevens', *I. opaca*, and *I.* × 'China Girl', pigment content gradually increased from 0 to 100 mM and peaked at 100 mM, with the largest increase observed in *I.* × 'China Girl' (31.01%), followed by *I.* 'Nellie R. Stevens' (21.27%) and *I. opaca* (6.96%). In *I. cornuta* 'Dwarf Burfordii'

and ‘Luteacarpus’, pigment content gradually increased from 0 to 150 mM and peaked at 150 mM, with increases of 6.58% and 5.00%, respectively, followed by a gradual decline from 200 to 250 mM, with decreases of 10.79% and 2.35% at 250 mM compared with 150 mM. *I.* × *cassine* showed a 6.65% increase at 50 mM compared with 0 mM, followed by a continuous decline thereafter, with a 16.73% decrease at 250 mM compared with 50 mM (**Fig. 3D**). Chl *a* showed no significant treatment effects in ‘Luteacarpus’ and *I.* × ‘*China Girl*’, but increased then decreased with rising salt concentration in the other five germplasms. Chl *b* showed greater variation among germplasms than Chl *a*, with six germplasms (except ‘Luteacarpus’) exhibiting a unimodal pattern—either increasing then decreasing or showing a sustained decline. In contrast, for Car, *I. opaca*, *I.* ‘Nellie R. Stevens’, *I. cornuta* ‘Dwarf Burfordii’, and *I.* × ‘China Girl’ showed an initial decrease followed by an increase with increasing treatment concentration, while *I.* × *cassine* and *I. dabieshanensis* showed a gradual increase (**Fig. 3A–C**).

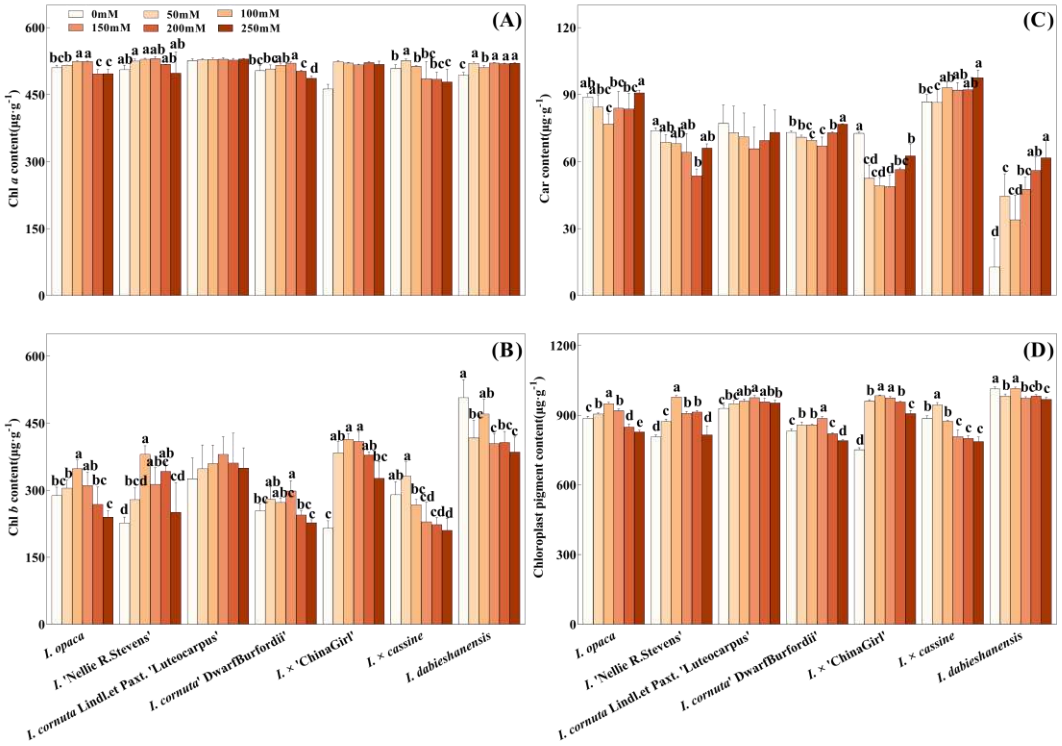


Fig. 3. Changes in chloroplast pigment content in seven *Ilex* germplasms under salt stress. Chl *a*, chlorophyll a; Chl *b*, chlorophyll b; Car, carotenoids. Same abbreviations apply to all tables and figures below.

3.2 Comprehensive analysis of salt tolerance in seven Ilex germplasms

3.2.1 Salt injury index

After 30 days of salt treatment, salt injury symptoms in the seven *Ilex* germplasms intensified with increasing NaCl concentration (**Table 3**). *I. opaca* showed the strongest salt tolerance, while *I.* × 'China Girl' was the most sensitive. At 0 mM, all germplasms grew normally. At 50 mM, only *I.* × *cassine* and *I.* × 'China Girl' showed slight leaf tip yellowing. At 100 mM, symptom differentiation became evident among germplasms, with some showing scorch, brown spots, or defoliation. At 150 mM, old leaf abscission and a few deaths occurred in certain germplasms. At 200 mM, half of the *I.* × 'China Girl' plants died, and other germplasms showed aggravated symptoms. At 250 mM, *I.* × *cassine* and *I. dabieshanensis* were severely damaged; while *I.* 'Nellie R. Stevens', *I. cornuta* 'Dwarf Burfordii', *I. cornuta* Lindl. et Paxt. 'Luteacarpus', and *I. opaca*

showed relatively mild symptoms, with *I. opaca* being the least affected.

Table 3. Leaf salt injury level and salt injury index of seven *Ilex* germplasms under salt stress

Breed	Salt injury level						Salt injury index (%)					
	0mM	50mM	100mM	150mM	200mM	250mM	0mM	50mM	100mM	150mM	200mM	250mM
I. 'Nellie R.Stevens'	0	1	1	2	3	4	0.00	1.79	8.93	25.00	40.18	53.57
I. cornuta 'Dwarf Burfordii'	0	1	2	2	2	4	0.00	2.68	8.93	26.79	17.86	53.57
I.×cassine	0	2	3	4	5	6	0.00	12.50	21.43	42.86	62.50	75.00
I. dabieshanensis	0	1	3	4	5	6	0.00	2.68	16.07	53.57	71.43	75.00
I. cornuta Lindl. et Paxt. 'Luteacarpus'	0	1	2	2	3	3	0.00	2.95	7.14	25.00	40.18	42.86
I. opaca	0	1	1	2	2	3	0.00	6.25	8.93	21.43	25.00	40.18
I. × 'China Girl'	0	2	4	5	6	6	0.00	10.71	21.43	40.18	69.64	80.36

3.2.2 Correlation analysis of physiological indicators

Pearson correlation analysis was conducted to examine the relationships among physiological traits of the seven *Ilex* germplasms under salt stress (Table 4). SI showed strong associations with several stress-responsive parameters, exhibiting negative relationships with Pn, Tr, and Gs, but a positive association with MDA ($p < 0.01$). A significant positive relationship was also observed between SI and Pro ($p < 0.05$). Photosynthetic traits displayed coordinated responses, with Pn closely associated with both Gs and Tr, while Gs was positively linked to Tr. In addition, Ci showed positive associations with Tr and Gs. For membrane stability and pigment-related traits, MDA was positively associated with Chl *b* but negatively associated with Car, whereas its relationship with Chl *a* was not significant. Among osmotic adjustment substances, SP exhibited a negative association with Pro, while no significant relationship was observed between SP and SI. SS showed positive associations with Chl *a* and Gs.

Table 4. Pearson correlation analysis of physiological parameters in seven *Ilex* germplasms under salt stress.

Index	SI	MDA	Chl *a*	Chl *b*	Car	SS	SP	Pro	Pn	Tr	Gs	Ci
SI	1.000											
MDA	0.457**	1.000										
Chl *a*	-0.138	0.304	1.000									
Chl b	0.025	0.667**	0.559*	1.000								
Car	-0.020	-0.620**	-0.240	-0.811**	1.000							
SS	-0.001	0.017	0.336*	0.08	0.133	1.000						
SP	0.001	0.248	0.288	0.081	0.109	0.002	1.000					
Pro	0.198	-0.113	0.012	0.206	-0.264	0.006	-0.730**	1.000				
Pn	-0.852**	-0.277	0.200	0.150	-0.200	0.024	-0.064	-0.062	1.000			
Tr	-0.616**	-0.188	0.306*	0.127	0.050	0.192	0.137	-0.130	0.622**	1.000		
Gs	-0.623**	-0.205	0.477**	0.226	-0.049	0.321*	0.094	-0.027	0.558**	0.749**	1.000	
Ci	-0.128	-0.105	-0.163	-0.103	0.126	0.145	0.024	0.079	0.106	0.417**	0.316*	1.000

Note: *p < 0.05, **p < 0.01, ***p < 0.001. The following abbreviations are used: SI, salt injury index; Pn, net photosynthetic rate; Gs, stomatal conductance; Ci, intercellular CO_2 concentration; and Tr, transpiration rate. The same abbreviations apply below for all figures and tables.

3.2.3 Random forest analysis of salt tolerance indicators

Based on the random forest model, the importance of each physiological indicator in explaining SI was analyzed (**Fig. 4**). Model parameters and accuracy results are detailed in **Supplementary Tables S2**. The model demonstrated satisfactory predictive performance on both the training and test sets, confirming its reliability. The contribution of each indicator to SI varied considerably. Among them, Pn showed the highest importance, accounting for 59.3% of the variance in SI across treatments, followed by Tr and Gs, which explained 13.6% and 9.4% of the variance, respectively. In addition, MDA alone accounted for 6.2% of the variance, while the remaining seven indicators collectively explained 11.44% of the variance.

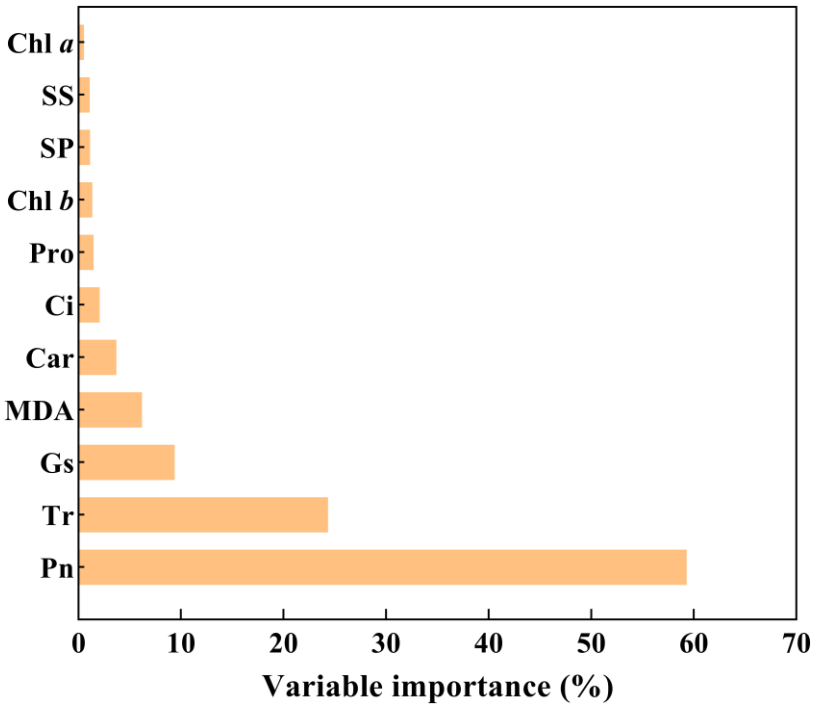


Fig. 4. The contribution of various physiological indicators to the salt damage index of holly.

3.2.4 Membership function values and comprehensive evaluation

According to the integrated membership scores, the seven Ilex germplasms exhibited a descending order of salt tolerance as follows: *I. opaca* > *I. cornuta* Lindl. et Paxt. 'Luteacarpus' > *I.* 'Nellie R. Stevens' > *I.* × 'China Girl' > *I. cornuta* 'Dwarf Burfordii' > *I.* × *cassine* > *I. dabieshanensis* (**Table 5**).

Table 5. Membership function values and comprehensive evaluation of seven *Ilex* germplasms under salt stress

Breed	SI	MDA	Chl *a*	Chl *b*	Car	SS	SP	Pro	Pn	Tr	Gs	Ci	Mean	Rank
I. opaca	0.750	0.836	0.718	0.280	0.848	0.800	0.573	0.237	0.608	0.693	0.728	0.578	0.637	1
I. cornuta Lindl. et Paxt. 'Luteacarpus'	0.694	0.464	0.969	0.484	0.693	0.676	0.861	0.065	0.491	0.583	0.529	0.475	0.582	2
I. 'Nellie R.Stevens'	0.694	0.642	0.812	0.298	0.624	0.554	0.720	0.155	0.745	0.600	0.653	0.439	0.578	3
I. × 'China Girl'	0.361	0.647	0.707	0.486	0.522	0.577	0.140	0.813	0.490	0.504	0.538	0.554	0.528	4
I. cornuta 'Dwarf Burfordii'	0.694	0.872	0.642	0.177	0.695	0.071	0.617	0.306	0.490	0.513	0.525	0.505	0.509	5
I.×cassine	0.444	0.867	0.542	0.163	0.927	0.221	0.611	0.308	0.326	0.408	0.465	0.626	0.492	6
I. dabieshanensis	0.472	0.160	0.759	0.746	0.353	0.171	0.680	0.238	0.512	0.461	0.540	0.462	0.463	7

3.3 Transcriptomic analysis of I. dabieshanensis under salt stress

3.3.1 Quality assessment of transcriptome sequencing data and identification of differentially expressed genes

To investigate the effects of salt stress on photosynthesis in *I. dabieshanensis*, RNA-seq analysis was performed using leaf samples sampled at six time points spanning the control condition and 3–24 h after NaCl treatment. After read preprocessing and genome mapping, 40,042 expressed genes were retained for downstream analyses. PCA separated the transcriptomic profiles among different treatment stages, with PC1 and PC2 explaining 71.28% and 14.45% of the overall variation, respectively (85.73% in total). (**Fig. 5A**). The correlation clustering heatmap further confirmed high correlations among samples within the same treatment group, whereas correlations among different treatment groups were relatively low (**Fig. 5B**). A time-dependent increase in DEG abundance was observed across the five salt treatment comparisons (3, 6, 9, 12, and 24 h vs CK) (Fig. 5C). The earliest response at 3 h involved 998 DEGs, including 757 induced and 241 repressed genes, whereas the 24 h treatment resulted in the strongest transcriptional alteration, with 2,841 DEGs (1,508 up-regulated and 1,333 down-regulated). Venn analysis identified 175 common DEGs that were differentially expressed at all time points (**Fig. 5D**); volcano plots showing the overall distribution of DEGs across the five comparison groups are presented in **Supplementary Fig. S1**.

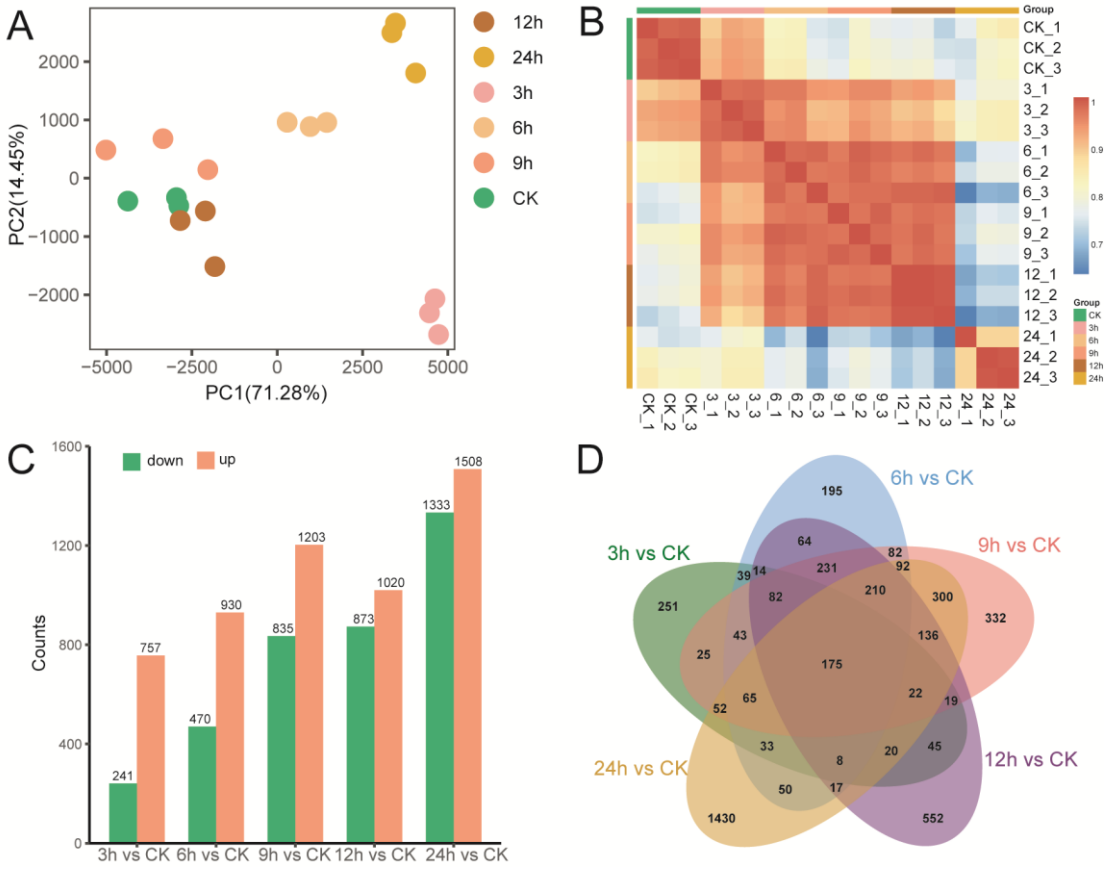


Fig. 5. Transcriptomic responses of *I. dabieshanensis* to salt stress. (A) PCA plot of 18 transcriptome samples. (B) Sample correlation heatmap illustrating transcriptomic relationships among 18 samples. (C) Numbers of up- and down-regulated DEGs identified in five comparisons (3 h vs CK, 6 h vs CK, 9 h vs CK, 12 h vs CK, and 24 h vs CK). (D) Venn diagram displaying shared and unique DEGs among the five comparison groups.

3.3.2 GO functional and KEGG pathway enrichment analysis of differentially expressed genes

A total of 4,987 DEGs were obtained from the five pairwise comparisons. Functional annotation showed that these genes were mainly associated with biological processes such as response to alcohol (21.9%), response to karrikin (21.8%), negative regulation of abscisic acid-activated signaling pathway (14.3%), auxin transport (4.5%), cellular response to phosphate starvation (3.2%), circadian rhythm (2.5%), and photosynthesis (2.5%) (Fig. 6A; Supplementary Table S3).

KEGG analysis indicated that the identified DEGs were primarily involved in glutathione metabolism, plant hormone signal transduction, MAPK signaling pathway–plant, carbon metabolism, carbon fixation in photosynthetic organisms, and photosynthesis–antenna proteins

(Fig. 6B; Supplementary Table S4). To further characterize the temporal changes in functional responses, enrichment analyses were conducted separately for DEGs detected at each sampling stage (3, 6, 9, 12, and 24 h vs CK), and the five most significant pathways from each comparison were summarized (Fig. 6C–D; Supplementary Tables S5 and S6).

Photosynthesis-associated GO categories, including photosynthesis, light harvesting, chlorophyll binding, and red/far-red light signaling, were consistently represented during the early response period (3–12 h). In contrast, genes altered at 24 h showed stronger associations with hormone-related processes, including regulation of abscisic acid-activated signaling pathway and regulation of response to alcohol. Similarly, KEGG analysis demonstrated that photosynthesis–antenna proteins, plant circadian rhythm, and plant hormone signal transduction were commonly affected across multiple time points, whereas carbon fixation in photosynthetic organisms and carbon metabolism became prominent mainly at 24 h.

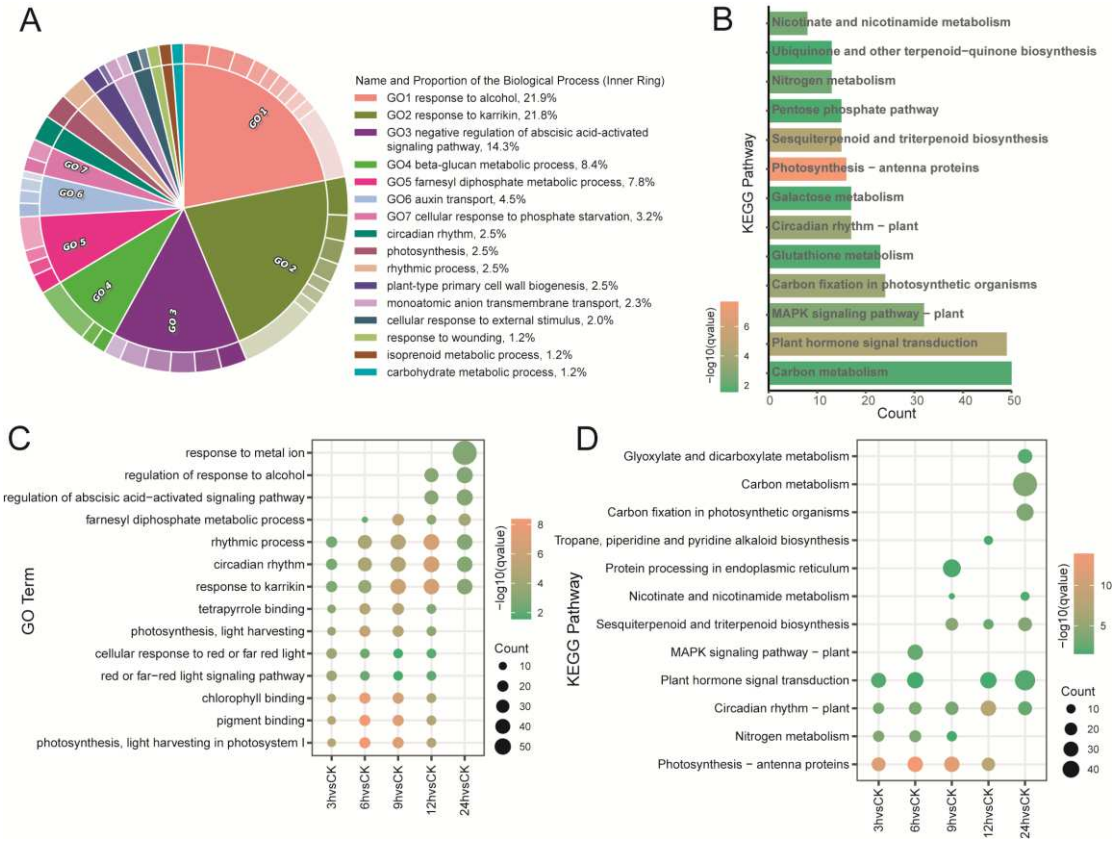


Fig. 6. Enrichment analysis of DEGs in response to salt stress. (A) Circle plot of GO enrichment for 4,987 DEGs. (B) Bar plot of KEGG pathway enrichment; color intensity indicates enrichment significance (-$\log_{10}$(q-value)). (C–D) Bubble plots of GO (C) and KEGG (D) enrichment across five comparison groups. Dot size reflects gene count; color indicates -$\log_{10}$(q-value).

3.3.3 Expression pattern analysis of key differentially expressed genes involved in photosynthesis

To gain further insight into the expression dynamics of photosynthesis-related genes, we extracted the corresponding DEGs from the GO and KEGG enrichment results and visualized their expression profiles using heatmaps (**Fig. 7A, 7B**). Among the four photosynthesis-related GO terms, the 11 DEGs involved in photosynthesis, light harvesting in photosystem I and chlorophyll binding—which encode photosystem I antenna complex and chlorophyll-binding proteins—generally exhibited an initial upregulation followed by a subsequent downregulation, with relatively high expression at 6 h and a gradual decline thereafter, returning to levels close to those of the control at 24 h. For the red/far-red light signaling pathway, six out of the 11 DEGs (e.g., ILEXP_LOCUS4880 and ILEXP_LOCUS21749) were markedly induced at 3–9 h, but their

expression decreased at 12–24 h. In the KEGG Photosynthesis – antenna proteins pathway, most antenna protein genes displayed a similar expression pattern, with early upregulation and later sustained downregulation, reaching the lowest levels at 24 h. In the Carbon fixation in photosynthetic organisms pathway, 12 DEGs (e.g., ILEXP_LOCUS19855 and ILEXP_LOCUS27326) showed relatively minor changes at early time points but were significantly upregulated at 24 h, whereas other genes (e.g., ILEXP_LOCUS2685, ILEXP_LOCUS3026, and ILEXP_LOCUS21504) exhibited continuous downregulation, reaching their minimum expression levels at 24 h.

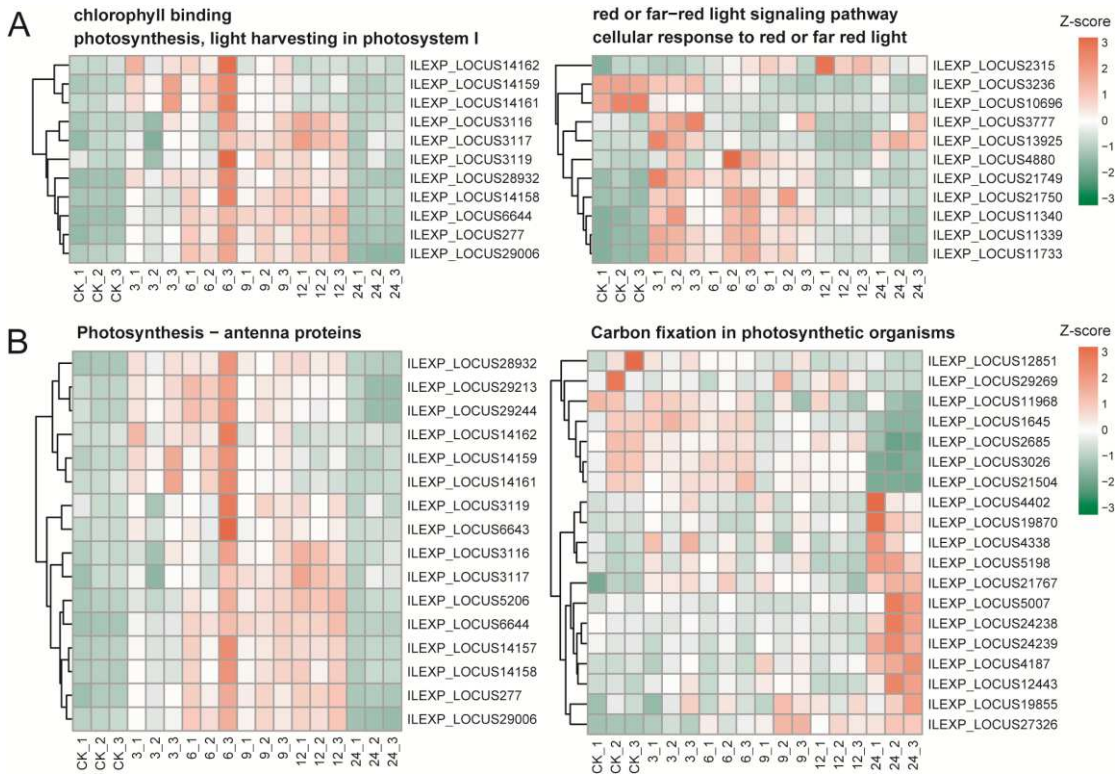


Fig. 7. Heatmap showing expression patterns of photosynthesis-related DEGs enriched in GO terms and KEGG pathways.

3.3.4 Enrichment of photosynthetic carbon fixation pathways

The temporal dynamics of GO and KEGG enrichment analyses indicated that salt stress progressively shifted the photosynthetic response from light harvesting towards carbon

assimilation. Notably, “Carbon fixation in photosynthetic organisms” was the only pathway significantly enriched at 24 h, suggesting a specific perturbation of carbon fixation under prolonged stress, prompting further analysis of this pathway.

Pathway analysis revealed that salt stress broadly affected genes encoding Calvin cycle enzymes (**Fig. 8**), including RBC, GAPC, and FBA. Among these, ILEXP_LOCUS4338 *(RBC)*, two *GAPC* genes (ILEXP_LOCUS4187 and ILEXP_LOCUS27326), and ILEXP_LOCUS5007 (*FBA*) showed minor changes at 3–12 h but were markedly upregulated at 24 h. Genes involved in RuBP regeneration were also regulated: ILEXP_LOCUS2685 (*SBPASE*) and ILEXP_LOCUS3026 (*RPI*) were progressively downregulated with prolonged stress, whereas two *PRK* genes (ILEXP_LOCUS24238 and ILEXP_LOCUS24239) were significantly upregulated at 24 h. Most Calvin cycle-related genes (e.g., ILEXP_LOCUS4187, ILEXP_LOCUS5007, ILEXP_LOCUS5198, ILEXP_LOCUS24238, ILEXP_LOCUS24239) exhibited limited changes at early stages but significant alterations at 24 h, with some continuously suppressed (e.g., ILEXP_LOCUS1645, ILEXP_LOCUS12851, ILEXP_LOCUS29269).

Additionally, C_4/CAM-related enzymes (PPC, MDH, NADP-ME, and ALAAT) were also affected. Two *PPC* genes (ILEXP_LOCUS19870 and ILEXP_LOCUS19855) were upregulated from 9 h onwards and peaked at 24 h, whereas two *MDH* genes (ILEXP_LOCUS11968 and ILEXP_LOCUS21504) were continuously downregulated over time. *HCEF1* (ILEXP_LOCUS5198), a regulator of photosynthetic electron transport, showed minor changes at 3–12 h but was strongly upregulated at 24 h.

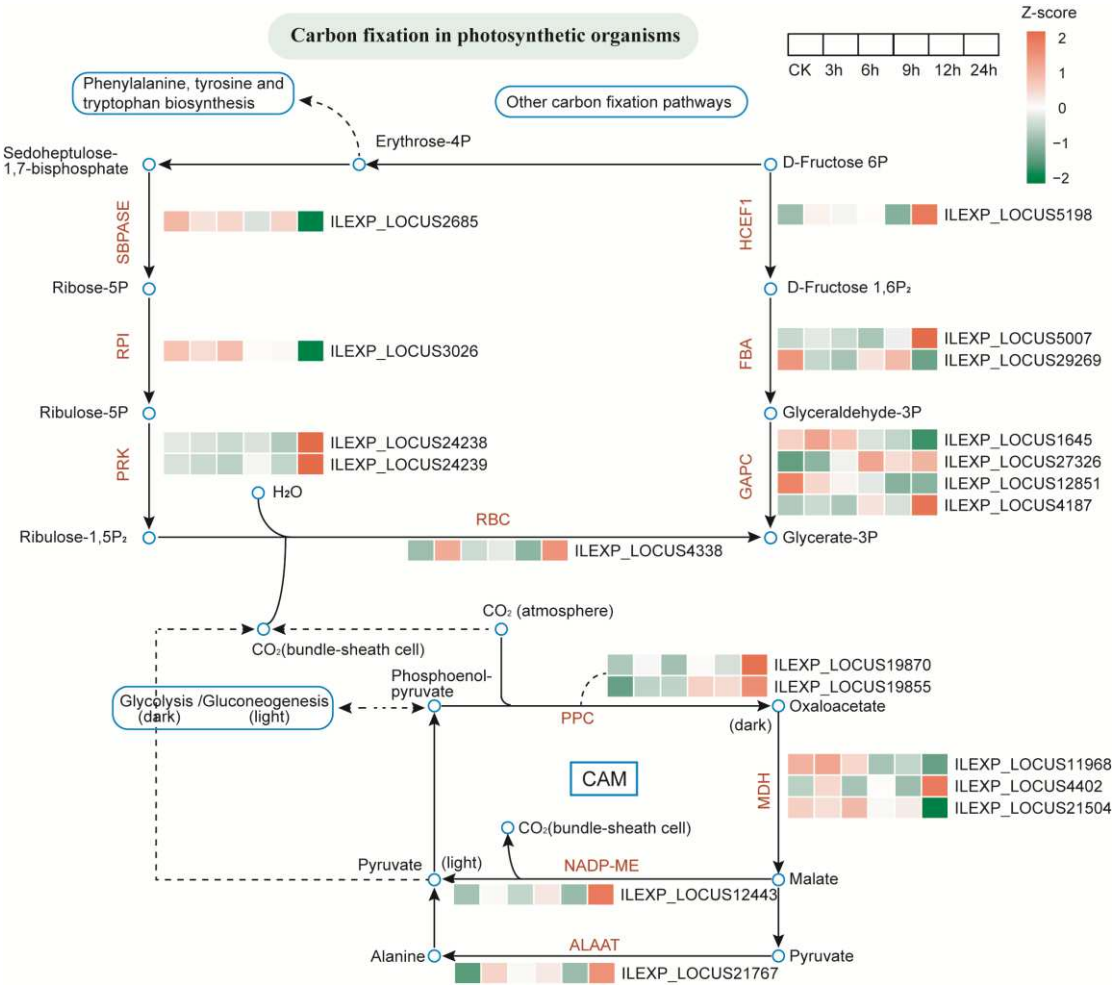


Fig. 8. Salt-induced changes in the carbon fixation pathway and associated DEGs. DEGs were projected onto the KEGG map of photosynthetic carbon fixation. The heatmap shows mean Z-scored expression values of DEGs linked to each enzymatic step across CK and salt treatments (3, 6, 9, 12, and 24 h). Enzyme abbreviations: ALAAT, alanine aminotransferase; NADP-ME, NADP-malic enzyme; MDH, malate dehydrogenase; PPC1, phosphoenolpyruvate carboxylase; RBC, ribulose bisphosphate carboxylase; GAPC, glyceraldehyde-3-phosphate dehydrogenase; FBA, fructose-bisphosphate aldolase; HCEF1, high cyclic electron flow 1; SBPASE, sedoheptulose-bisphosphatase; RPI, ribose-5-phosphate isomerase; PRK, phosphoribulokinase.

4. Discussion

4.1 Significant interspecific variation in salt tolerance among the seven Ilex germplasms

Plant growth and development are severely constrained by salt stress, which imposes osmotic imbalance, ionic toxicity, and oxidative damage [8, 37, 38]. In this study, the salt injury index of the seven *Ilex* germplasms increased significantly with rising NaCl concentration, with marked differences among germplasms, indicating substantial interspecific variation in salt tolerance

within the genus. Membership function analysis integrating multiple physiological indicators effectively differentiated the salt tolerance of the seven *Ilex* germplasms, with the rankings consistent with observed physiological trends. This confirmed the applicability of this method for salt tolerance evaluation in *Ilex*. Similarly, [39] demonstrated that this multi-indicator approach effectively discriminates interspecific salt tolerance in *Ilex*; their principal component analysis identified salt injury index, relative electrical conductivity, MDA, soluble protein, and chlorophyll as core indicators, whereas our random forest analysis highlighted Pn, Gs, and Tr as major contributors to salt injury variation. Although the key indicators differed, both studies emphasized the value of multi-indicator evaluation. The greater importance of photosynthetic parameters in our study may relate to earlier measurements (day 7), which likely captured rapid photosynthetic responses.

Interspecific differences in salt tolerance are shaped by genetic background and ecological adaptive history. *I. dabieshanensis*, endemic to the Dabie Mountains, occurs in acidic red soils with extremely low soluble salt content; prolonged adaptation may have led to adaptive degradation of its salt stress response pathways [40]. In contrast, Yu et al. [41] found that the coastal species *I. integra* accumulated less Na^+ and exhibited stronger antioxidant capacity than the inland I. purpurea. Similarly, *I. opaca*, native to the eastern coast of North America, showed strong salt tolerance, supporting the influence of ecological origin on salt tolerance. Salt tolerance variation among germplasms thus reflects the integrated performance of ion homeostasis, photosynthetic regulation, and antioxidant defense [42, 43]. Hence, a thorough assessment of salt tolerance mechanisms in *Ilex* should incorporate morphological, physiological, and molecular dimensions.

4.2 Synergistic roles of membrane lipid peroxidation and osmotic regulation in salt acclimation of Ilex

Membrane lipid peroxidation, indicated by MDA accumulation, is a reliable marker of salt-induced membrane damage [44, 45]. In this study, MDA content increased with rising NaCl concentration, with the highest levels recorded in *I. dabieshanensis*, suggesting the greatest membrane impairment in this species. By contrast, salt-tolerant taxa such as *I. opaca* maintained lower MDA levels, indicative of superior membrane stability. The negative correlation between MDA and carotenoid content implies a protective role of carotenoids in photoprotection and ROS scavenging [4], and their stability appears critical for maintaining photosynthetic membrane integrity.

Regarding osmotic regulation, SS, SP, and Pro exhibited a unimodal response to increasing salinity, characterized by an initial increase under moderate stress followed by a decline under high salinity. This pattern indicates that low salinity promotes osmolyte accumulation to reduce osmotic potential, whereas high salinity suppresses their synthesis or accelerates their degradation. Osmotic adjustment strategies differed markedly among germplasms. For instance, *I.* 'Nellie R. Stevens', primarily accumulated soluble sugars (SS reached 78.02 $mg \cdot g^{-1}$ at 150 mM NaCl). Although energetically costly (~50–70 M ATP per M solute [46]), soluble sugars also function in antioxidant protection and carbon storage, offering additional physiological benefits [47]. In contrast, *I.* × 'China Girl' showed strong reliance on proline accumulation (65.70% increase), consistent with reports in woody plants such as *Casuarina equisetifolia*, which rapidly synthesizes proline as a major compatible solute under salt stress, with foliar proline content strongly correlated with Na^+ concentration [48]. Proline also functions as a non-enzymatic ROS scavenger,

playing dual roles in osmotic and oxidative defense [49]. The negative correlation between Pro and SP ($r = -0.730$) suggests that proline accumulation may occur at the expense of soluble protein degradation [46], while the positive correlation between Pro and salt injury index implies that proline content may reflect stress severity rather than tolerance capacity [50]. Collectively, these findings indicate that the seven *Ilex* germplasms adopted differentiated osmotic adjustment strategies, reflecting an adaptive trade-off between osmotic adjustment efficiency and energy expenditure.

4.3 Photosynthetic inhibition as a key physiological process underlying salt injury in Ilex

Salt stress affects photosynthesis through both stomatal and non-stomatal limitations. In this study, Pn was significantly positively correlated with Gs, indicating that stomatal closure is a primary factor contributing to reduced photosynthetic performance by limiting CO_2 availability. Under progressive salt stress, Ci either initially increased and then decreased or remained elevated in salt-sensitive germplasms, suggesting a gradual shift from stomatal to non-stomatal limitations, such as reduced mesophyll conductance and decreased Rubisco carboxylation efficiency [16]. The relative contribution of these two limitations jointly determines the overall stability of photosynthesis among germplasms [50].

Non-stomatal limitations reflect underlying damage to photosynthetic structure and function. A prominent response observed in this study was the decline in chlorophyll and carotenoid contents with increasing salinity, consistent with previous reports [51, 52]. The transient increase in pigment content under low salinity in some germplasms may be attributed to reduced leaf expansion leading to higher chloroplast density per unit leaf area [53]. However, with increasing salt stress, pigment degradation accelerated, with Chl *a* exhibiting greater sensitivity than Chl *b* [6]. Carotenoids,

beyond their role in light harvesting, are essential for photoprotection and ROS scavenging, and are generally positively associated with salt tolerance [5]. In this study, the salt-tolerant *I. opaca* maintained relatively stable carotenoid levels, whereas the salt-sensitive *I. dabieshanensis* showed a marked decline, consistent with observations in other salt-sensitive woody species [54]. In addition, salt-induced chloroplast structural damage, such as thylakoid disorganization and plastoglobuli accumulation, may further constrain light capture and energy conversion efficiency [55].

At the level of electron transport and carbon assimilation, salt-tolerant germplasms maintained higher photochemical efficiency and electron transport capacity, whereas PSII efficiency declined markedly in salt-sensitive germplasms under increasing salinity [15, 56]. Moreover, salt stress inhibits Rubisco activity and Rubisco activase function and suppresses the expression of Calvin cycle-related genes, thereby restricting carbon fixation at the biochemical and transcriptional levels [17]. In the present study, salt-tolerant germplasms maintained relatively higher Pn and Gs under high salinity, whereas *I. dabieshanensis* exhibited the most pronounced reductions, indicating that its photosynthetic apparatus is impaired at multiple levels, including stomatal regulation, pigment stability, electron transport, and carbon assimilation.

Consistently, random forest analysis identified Pn as the dominant contributor to salt injury variation (59.3%), far exceeding Gs (9.4%) and Tr (13.6%), highlighting photosynthetic capacity as a core trait for evaluating salt tolerance in *Ilex*. Overall, salt-tolerant germplasms display coordinated advantages in stomatal regulation, pigment maintenance, and carbon fixation, whereas *I. dabieshanensis* is compromised across multiple components of the photosynthetic machinery. These results suggest that the maintenance of stable photosynthetic performance, particularly

pigment integrity, efficient stomatal regulation, and robust electron transport, is a key physiological basis underlying salt tolerance in *Ilex* species.

4.4 Transcriptomic analysis reveals molecular mechanisms of photosynthetic inhibition in I. dabieshanensis

Physiological evaluation identified *I. dabieshanensis* as the most salt-sensitive germplasm among the seven *Ilex* germplasms tested; we therefore performed a time-series transcriptomic analysis on leaves of this species under 200 mM NaCl treatment. Temporal dynamics of GO and KEGG enrichment analyses revealed a hierarchical progression of photosynthetic inhibition from light reactions to carbon assimilation: at early stages (3–12 h), the transcriptional response was dominated by genes involved in light harvesting, chlorophyll binding, and light signaling, whereas after 24 h, the regulatory focus shifted toward ABA signaling and stress defense pathways, indicating a strategic transition from photosynthetic maintenance to stress survival. This pattern is consistent with reports that photosynthetic pathways are more sensitive to stress than other basal biological processes in rice [57], and with the coordinated changes in hormone signaling and carbon metabolism observed in Astragalus cicer under salt stress [58]. KEGG analysis further revealed that the "Photosynthesis – antenna proteins" pathway was significantly enriched at all time points, whereas "Carbon fixation" reached significance only at 24 h, indicating that salt stress first attacks the light-harvesting antenna complexes and subsequently extends to the carbon fixation network, a finding consistent with the conclusion that the PSII is the most vulnerable component of the photosynthetic apparatus to salt-induced damage in melon [59]. Antenna protein genes exhibited transient upregulation at 6 h followed by sustained downregulation at 24 h, suggesting that the initial compensatory response is suppressed under prolonged stress. The

time-specific enrichment of the carbon fixation pathway suggested that this process may represent the ultimate convergence node of salt-induced damage to the photosynthetic apparatus; we therefore further analyzed the expression dynamics of genes encoding key enzymes in this pathway. Within the carbon fixation pathway, Calvin cycle enzyme genes exhibited differentiated expression: genes encoding RBC, GAPC, and FBA showed limited changes at early stages but were significantly upregulated at 24 h, whereas *SBPASE* and *RPI* were progressively downregulated with prolonged stress. This expression divergence indicates that long-term salt stress does not simply suppress carbon fixation uniformly, but rather reshapes the carbon assimilation network by differentially modulating distinct metabolic nodes to optimize carbon flux allocation and energy balance. By contrast, in the halophyte *Nitraria sibirica*, salt stress upregulates the expression of genes encoding RuBisCO large chain, malate dehydrogenase, and other key carbon fixation enzymes through ethylene signaling, thereby enhancing photosynthesis and promoting growth [60], indicating that the direction of carbon metabolic reprogramming may vary depending on the species' intrinsic salt tolerance strategy. Similar reprogramming of carbon metabolism has been documented in salt-tolerant sweet sorghum [61], saline-alkali-stressed mung bean [62], and drought-stressed Shanlan upland rice [63], indicating that complex modulation of carbon fixation represents a conserved adaptive strategy across plant species under abiotic stress.

Furthermore, differential expression was also detected for C_4/CAM-related enzymes (PPC, MDH, NADP-ME, ALAAT): two PPC genes were upregulated from 9 h onward and peaked at 24 h, whereas two MDH genes were continuously downregulated. The induction of C_4/CAM-related genes in a C_3 plant may represent an adaptive mechanism to enhance organic acid metabolism and carbon skeleton redistribution. This contrasts with the finding in the

halophyte Nitraria sibirica, where salt stress stimulated carbon fixation through ethylene signaling [60]: carbon fixation was promoted in the halophyte, whereas in the glycophytic *I. dabieshanensis* it was predominantly inhibited, with only partial compensatory induction of certain metabolic enzymes. The differential expression of HCEF1 suggested that the plant may attempt to adjust electron transport efficiency to balance the energy demand between light reactions and carbon assimilation, but this adjustment appears insufficient to offset the overall decline in photosynthetic performance.

In summary, our transcriptomic analysis suggests that salt-induced photosynthetic inhibition in I. dabieshanensis may involve multi-layered responses, ranging from early light-harvesting adjustments to late carbon fixation network remodeling and hormone-driven defense. The progressive inhibition of the Calvin cycle, together with compensatory attempts through C_4-like enzyme induction, may collectively lead to metabolic imbalance and consequently constrain photosynthetic carbon assimilation efficiency.

5. Conclusion

This study provides a physiological and molecular characterization of salt stress responses in seven evergreen *Ilex* germplasms, with a focus on the most salt-sensitive accession. Considerable interspecific variation was evident in stress tolerance, with *I. opaca* showing superior photosynthetic performance and lower salt injury, coupled with maintained osmotic and pigment homeostasis under high salinity. In contrast, *I. dabieshanensis* displayed the greatest photosynthetic decline and the highest MDA accumulation and salt injury. Correlation and random forest analyses identified Pn, Tr, and Gs as the primary contributors to salt injury variation,

accounting for 82.3% of the total variance (Pn alone: 59.3%). Transcriptomic profiling of *I. dabieshanensis* revealed significant downregulation of photosynthesis- and antenna protein-related genes. Time-course analysis further showed a progressive transcriptional shift from light harvesting to carbon assimilation under salt stress, with the carbon fixation pathway enriched exclusively under prolonged stress, and Calvin cycle genes displaying differential regulation rather than uniform repression. Together, these results define the physiological and molecular response patterns of evergreen *Ilex* germplasms to salinity, providing a basis for identifying salt-tolerant genotypes and supporting their use in saline-land greening.

Declarations

Ethics approval and consent to participate

Not applicable.

Consent for publication

Not applicable.

Availability of data and materials

The transcriptomic data analyzed in this study are publicly available in the NCBI BioProject database under accession number PRJNA1066056 and can be accessed via the following link: https://www.ncbi.nlm.nih.gov/bioproject/PRJNA1066056.

Funding

The research was supported by the State Key Laboratory of Subtropical Silviculture (SKLSS-KF2023-07), and the Scientific Fund of Nanjing Botanical Garden Mem. Sun Yat-Sen (JSPKLB202510).

Declaration of competing interest

The authors declare that they have no conflicts of interest.

Author contributions

B.L.: Conceptualization, Visualization, Writing – original draft, Writing – review & editing; X.C.: Data curation, Formal analysis; H.J.: Software; C.W.: Methodology; T.Z.: Investigation; B.Z.: Validation, Project administration; H.C.: Funding acquisition, Supervision, Resources, Writing – review & editing. All authors reviewed the manuscript.

Acknowledgements

Not applicable.

Reference

1. FAO: **Land and Plant Nutrition Management Service**. In.; 2008. http://www.fao.org/ag/agl/agll/spush/
2. Zhou H, Shi H, Yang Y, Feng X, Chen X, Xiao F, Lin H, Guo Y: **Insights into plant salt stress signaling and tolerance**. *Journal of Genetics and Genomics* 2024, **51**(1):16-34. https://doi.org/10.1016/j.jgg.2023.08.007
3. Shabala S, Wu H, Bose J: **Salt stress sensing and early signalling events in plant roots: Current knowledge and hypothesis**. *Plant Science* 2015, **241**:109-119. https://doi.org/10.1016/j.plantsci.2015.10.003
4. Shah SH, Houborg R, McCabe MF: **Response of Chlorophyll, Carotenoid and SPAD-502 Measurement to Salinity and Nutrient Stress in Wheat (Triticum aestivum L.)**. In: *Agronomy.* vol. 7; 2017: 61. https://doi.org/10.3390/agronomy7030061
5. Nagy Z, Daood H, Ambrózy Z, Helyes L: **Determination of Polyphenols, Capsaicinoids, and Vitamin C in New Hybrids of Chili Peppers**. *Journal of Analytical Methods in Chemistry* 2015, **2015**(1):102125. https://doi.org/10.1155/2015/102125
6. Acosta-Motos JR, Ortuño MF, Bernal-Vicente A, Diaz-Vivancos P, Sanchez-Blanco MJ, Hernandez JA: **Plant Responses to Salt Stress: Adaptive Mechanisms**. In: *Agronomy.* vol. 7; 2017: 18. https://doi.org/10.3390/agronomy7010018
7. Deshmukh Y, Khare P: **Effect of Salinity Stress on Growth Parameters and Metabolites of Medicinal Plants: a Review**. In.; 2017: 197-234. https://doi.org/10.1201/9781315365992-9
8. Shabala S, Munns R: **Salinity stress: Physiological constraints and adaptive mechanisms**. *Plant Stress Physiology* 2012, **59–93**:59-93. https://doi.org/10.1079/9781845939953.0059
9. Yun F, Bose J, Zhou M, Sergey S: **ROS Production, Scavenging, and Signaling under Salinity Stress**. In.; 2015: 187-206. https://doi.org/10.1201/b19246-11
10. Cen H, Wang T, Liu H, Tian D, Zhang Y: **Melatonin Application Improves Salt Tolerance of Alfalfa (Medicago sativa L.) by Enhancing Antioxidant Capacity**. In: *Plants.* vol. 9; 2020: 220. https://doi.org/10.3390/plants9020220
11. Yang Y, Guo Y: **Elucidating the molecular mechanisms mediating plant salt-stress**

responses. *New Phytologist* 2018, **217**(2):523-539. https://doi.org/10.1111/nph.14920

12. Gill SS, Tuteja N: **Reactive oxygen species and antioxidant machinery in abiotic stress tolerance in crop plants**. *Plant Physiology and Biochemistry* 2010, **48**(12):909-930. https://doi.org/10.1016/j.plaphy.2010.08.016

13. Kovtun Y, Chiu W-L, Tena G, Sheen J: **Functional analysis of oxidative stress-activated mitogen-activated protein kinase cascade in plants**. *Proceedings of the National Academy of Sciences* 2000, **97**(6):2940-2945. https://doi.org/10.1073/pnas.97.6.2940

14. Ryu H, Cho Y-G: **Plant hormones in salt stress tolerance**. *Journal of Plant Biology* 2015, **58**(3):147-155. https://doi.org/10.1007/s12374-015-0103-z

15. Li Q, Qin Y, Hu X, Li G, Ding H, Xiong X, Wang W: **Transcriptome analysis uncovers the gene expression profile of salt-stressed potato (Solanum tuberosum L.)**. *Scientific reports* 2020, **10**(1):5411. https://doi.org/10.1038/s41598-020-62057-0

16. Stefanov M, Yotsova E, Rashkov G, Ivanova K, Markovska Y, Apostolova EL: **Effects of salinity on the photosynthetic apparatus of two Paulownia lines**. *Plant Physiology and Biochemistry* 2016, **101**:54-59. https://doi.org/10.1016/j.plaphy.2016.01.017

17. Lee SY, Damodaran PN, Roh KS: **Influence of salicylic acid on rubisco and rubisco activase in tobacco plant grown under sodium chloride in vitro**. *Saudi Journal of Biological Sciences* 2014, **21**(5):417-426. https://doi.org/10.1016/j.sjbs.2014.04.002

18. Yao X, Song Y, Yang J-B, Tan Y-H, Corlett RT: **Phylogeny and biogeography of the hollies (Ilex L., Aquifoliaceae)**. 2021, **59**(1):73-82.https://doi.org/10.1111/jse.12567

19. Al-Habsi S, Percival G: **Sucrose-Induced Tolerance to and Recovery from Deicing Salt Damage in Containerized Ilex aquifolium L. and Quercus robur L**. *Arboriculture and Urban Forestry* 2006, **32**. https://doi.org/10.48044/jauf.2006.035

20. Yao X, Lu Z, Song Y, Hu X, Corlett RT: **A chromosome-scale genome assembly for the holly (Ilex polyneura) provides insights into genomic adaptations to elevation in Southwest China**. *Horticulture Research* 2022, **9**. https://doi.org/10.1093/hr/uhab049

21. Chen H, Li H, Chong X, Zhou T, Lu X, Wang X, Zheng B: **Transcriptome Analysis of the Regulatory Mechanisms of Holly (Ilex dabieshanensis) under Salt Stress Conditions**. 2024, **13**(12):1638. https://doi.org/10.3390/plants13121638

22. Zou YP, Huang YJ, Zhang DL, Chen H, Liang YW, Hao MZ, Yin YL: **Molecular Mechanisms of Chlorophyll Deficiency in Ilex attenuata 'Sunny Foster' Mutant**. *Plants-Basel* 2024, **13**(10). https://doi.org/10.3390/plants13101284

23. Yang Y, Liu S, Du G, Liu F, Tang K, Deng G, Li J, Jiang W: **Exogenous Application of Phytohormones Alleviates Salt Injury to Growth, Physiological, and Biochemical Attributes of Hemp Seedlings**. *Journal of Plant Growth Regulation* 2024, **43**(7):2439-2453. https://doi.org/10.1007/s00344-024-11278-y

24. Hodges DM, DeLong JM, Forney CF, Prange RK: **Improving the thiobarbituric acid-reactive-substances assay for estimating lipid peroxidation in plant tissues containing anthocyanin and other interfering compounds**. *Planta* 1999, **207**(4):604-611. https://doi.org/10.1007/s004250050524

25. Yemm EW, Willis AJ: **The estimation of carbohydrates in plant extracts by anthrone**. *Biochemical Journal* 1954, **57**(3):508-514. https://doi.org/10.1042/bj0570508

26. Shiba KS, Kanamori K, Harada T, Nakao M, Nakajima K, Kodaira T, Nakagawa H: **A cause of discrepancy between values for urinary protein as assayed by the Coomassie Brilliant Blue G-250 method and the sulfosalicylic acid method**. *Clinical Chemistry* 1985, **31**(7):1215-1218. https://doi.org/10.1093/clinchem/31.7.1215

27. Bates LS, Waldren RP, Teare ID: **Rapid determination of free proline for water-stress studies**. *Plant and Soil* 1973, **39**(1):205-207. https://doi.org/10.1007/BF00018060

28. Lichtenthaler HK: **[34] Chlorophylls and carotenoids: Pigments of photosynthetic biomembranes**. In: *Methods in Enzymology.* vol. 148: Academic Press; 1987: 350-382. https://doi.org/10.1016/0076-6879(87)48036-1

29. Chen S: **Ultrafast one-pass FASTQ data preprocessing, quality control, and deduplication using fastp**. *iMeta* 2023, **2**(2):e107. https://doi.org/10.1002/imt2.107

30. Kim D, Paggi JM, Park C, Bennett C, Salzberg SL: **Graph-based genome alignment and genotyping with HISAT2 and HISAT-genotype**. *Nature Biotechnology* 2019, **37**(8):907-915. https://doi.org/10.1038/s41587-019-0201-4

31. Liao Y, Smyth G, Shi W: **FeatureCounts: An efficient general purpose program for assigning sequence reads to genomic features**. *Bioinformatics (Oxford, England)* 2013, **30**.

https://doi.org/10.1093/bioinformatics/btt656

32. Cantalapiedra CP, Hernández-Plaza A, Letunic I, Bork P, Huerta-Cepas J: **eggNOG-mapper v2: Functional Annotation, Orthology Assignments, and Domain Prediction at the Metagenomic Scale**. *Molecular Biology and Evolution* 2021, **38**(12):5825-5829. https://doi.org/10.1093/molbev/msab293

33. Bu D, Luo H, Huo P, Wang Z, Zhang S, He Z, Wu Y, Zhao L, Liu J, Guo J *et al*: **KOBAS-i: intelligent prioritization and exploratory visualization of biological functions for gene enrichment analysis**. *Nucleic Acids Research* 2021, **49**(W1):W317-W325. https://doi.org/10.1093/nar/gkab447

34. Wu T, Hu E, Xu S, Chen M, Guo P, Dai Z, Feng T, Zhou L, Tang W, Zhan L *et al*: **clusterProfiler 4.0: A universal enrichment tool for interpreting omics data**. *The Innovation* 2021, **2**(3):100141. https://doi.org/10.1016/j.xinn.2021.100141

35. Xiu WY, Zhu Y, Chen B, Hu Y, Dawuda MM: **Effects of paclobutrazol on the physiological characteristics of Malus halliana Koehne Seedlings under drought stress via principal component analysis and membership function analysis**. *Arid Land Research and Management* 2019, **33**(1):97-113. https://doi.org/10.1080/15324982.2018.1488300

36. Li W, Wu W, Yu M, Tao H, Yao X, Cheng T, Zhu Y, Cao W, Tian Y: **Monitoring rice grain protein accumulation dynamics based on UAV multispectral data**. *Field Crops Research* 2023, **294**:108858. https://doi.org/10.1016/j.fcr.2023.108858

37. Munns R, Tester M: **Mechanisms of Salinity Tolerance**. 2008, **59**(Volume 59, 2008):651-681. https://doi.org/10.1146/annurev.arplant.59.032607.092911

38. Hasegawa PM, Bressan RA, Zhu J-K, Bohnert HJ: **PLANT CELLULAR AND MOLECULAR RESPONSES**. 2000, **51**(Volume 51, 2000):463-499. https://doi.org/10.1146/annurev.arplant.51.1.463

39. Liang C, Shi G, Jin X: **Response of Salt Stress on Growth and Physiological of Ilex Cultivars**. *Northern Horticulture* 2021(16):74-82. (in Chinese). https://doi.org/10.11937/bfyy.20210234

40. Gupta B, Huang B: **Mechanism of Salinity Tolerance in Plants: Physiological, Biochemical, and Molecular Characterization**. *International Journal of Genomics* 2014, **2014**(1):701596. https://doi.org/10.1155/2014/701596

41. Yu Y, Zhang M, Feng J, Sun S, Zhou P, Yang J: **Physiological analysis reveals relatively higher salt tolerance in roots of Ilex integra than in those of Ilex purpurea**. *Journal of Forestry Research* 2022, **33**(4):1187-1196. https://doi.org/10.1007/s11676-021-01386-w

42. Zhao S, Zhang Q, Liu M, Zhou H, Ma C, Wang P: **Regulation of Plant Responses to Salt Stress**. 2021, **22**(9):4609. https://doi.org/10.3390/ijms22094609

43. Khan I, Awan SA, Rizwan M, Hassan ZU, Akram MA, Tariq R, Brestic M, Xie W: **Nanoparticle's uptake and translocation mechanisms in plants via seed priming, foliar treatment, and root exposure: a review**. *Environmental Science and Pollution Research* 2022, **29**(60):89823-89833. https://doi.org/10.1007/s11356-022-23945-2

44. Gill SS, Tuteja N: **Reactive oxygen species and antioxidant machinery in abiotic stress tolerance in crop plants**. *Plant Physiology & Biochemistry* 2010, **48**(12):909-930. https://doi.org/10.1016/j.plaphy.2010.08.016

45. Sharma P, Jha AB, Dubey RS, Pessarakli M: **Reactive Oxygen Species, Oxidative Damage, and Antioxidative Defense Mechanism in Plants under Stressful Conditions**. *Journal of Botany* 2012, **2012**(1):217037. https://doi.org/10.1155/2012/217037

46. Shabala S, Shabala L: **Ion transport and osmotic adjustment in plants and bacteria**. *BioMolecular Concepts* 2011, **2**. https://doi.org/10.1515/BMC.2011.032

47. Gupta NK, Meena SK, Gupta S, Khandelwal SK: **Gas Exchange, Membrane Permeability, and Ion Uptake in Two Species of Indian Jujube Differing in Salt Tolerance**. *Photosynthetica* 2002, **40**(4):535-539. https://doi.org/10.1023/A:1024343817290

48. Tani C, Sasakawa H: **Proline accumulates in Casuarina equisetifolia seedlings under salt stress**. *Soil Science and Plant Nutrition* 2006, **52**(1):21-25. https://doi.org/10.1111/j.1747-0765.2006.00005.x

49. Aslamarz A, Vahdati K, Hassani D, Rahemi M, Mohamadi N, Leslie C: **Cold hardiness and its relationship with proline content in Persian walnut**. *European Journal of Horticultural Science* 2011, **76**:84-90. https://doi.org/10.1079/ejhs.2011/2593885

50. Ashraf M, Foolad MR: **Roles of glycine betaine and proline in improving plant abiotic stress resistance**. *Environmental and Experimental Botany* 2007, **59**(2):206-216. https://doi.org/10.1016/j.envexpbot.2005.12.006

51. Loreto F, Centritto M, Chartzoulakis K: **Photosynthetic limitations in olive cultivars with different sensitivity to salt stress**. *Plant, Cell & Environment* 2003, **26**(4):595-601. https://doi.org/10.1046/j.1365-3040.2003.00994.x

52. Deng L, Fukuda R, Kakihara T, Narita K, Ohta A: **Incorporation and remodeling of phosphatidylethanolamine containing short acyl residues in yeast**. *Biochimica et Biophysica Acta (BBA) - Molecular and Cell Biology of Lipids* 2010, **1801**(6):635-645. https://doi.org/10.1016/j.bbalip.2010.02.008

53. Sahu SM, Misra AN, Misra M, Ramaswamy NK, Desai TS: **Sodium Chloride Salt Stress Induced Changes in Thylakoid Pigment-Protein Complexes and Photosystem II Activity of Mungbean (Vigna Radiata l.) Seedlings**. In: *Photosynthesis: Mechanisms and Effects: Volume I–V: Proceedings of the XIth International Congress on Photosynthesis, Budapest, Hungary, August 17–22, 1998.* Edited by Garab G. Dordrecht: Springer Netherlands; 1998: 2625-2628. https://doi.org/10.1007/978-94-011-3953-3_617

54. Lu Y, Zeng FJ, Li XY, Zhang B: **Physiological changes of three woody plants exposed to progressive salt stress**. *Photosynthetica* 2021, **59**(1):171-184. https://doi.org/10.32615/ps.2021.007

55. Li W: **Effect of Environmental Salt Stress on Plants and the Molecular Mechanism of Salt Stress Tolerance**. *International Journal of Environmental Sciences & Natural Resources* 2017, **7**. https://doi.org/10.19080/IJESNR.2017.07.555714

56. Dionisio-Sese ML, Tobita S: **Effects of salinity on sodium content and photosynthetic responses of rice seedlings differing in salt tolerance**. *Journal of Plant Physiology* 2000, **157**(1):54-58. https://doi.org/10.1016/S0176-1617(00)80135-2

57. Barzi SMA, Ahmadikhah A, Haghi R: **Comparative Transcriptome Analysis of Two Contrasting Rice Genotypes Reveals the Role of Photosynthesis, CO2 Fixation/Metabolism and MAPK Signaling Pathways in Response to Drought Stress**. *Journal of Plant Growth Regulation* 2026, **45**(2):1537-1552. https://doi.org/10.1007/s00344-025-11961-8

58. Zhang Y, Dong W, Ma H, Zhao C, Ma F, Wang Y, Zheng X, Jin M: **Comparative transcriptome and coexpression network analysis revealed the regulatory mechanism of Astragalus cicer**

L. in response to salt stress. *BMC Plant Biology* 2024, **24**(1):817. https://doi.org/10.1186/s12870-024-05531-5

59. Liu T, Amanullah S, Xu H, Gao P, Du Z, Hu X, Han M, Che Y, Zhang L, Qi G *et al*: **RNA-Seq Identified Putative Genes Conferring Photosynthesis and Root Development of Melon under Salt Stress**. In: *Genes.* vol. 14; 2023: 1728. https://doi.org/10.3390/genes14091728

60. Lu L, Wang Y, Chen Y, Zhu L, Wu X, Shi J, Chen J, Cheng T: **Salt stimulates carbon fixation in the halophyte Nitraria sibirica to enhance growth**. *Forestry Research* 2025, **5**(1):e004. https://doi.org/10.48130/forres-0025-0004

61. Sui N, Yang Z, Liu M, Wang B: **Identification and transcriptomic profiling of genes involved in increasing sugar content during salt stress in sweet sorghum leaves**. *BMC Genomics* 2015, **16**(1):534. https://doi.org/10.1186/s12864-015-1760-5

62. Zhu K, Li X, Xue R, Gao R, Zhang W, Bao H, Zong H: **Integrated transcriptomic and metabolomic identification of the core pathway of photosynthetic carbon fixation in mung bean under saline-alkali stress**. 2026, **Volume 17 - 2026**. https://doi.org/10.3389/fpls.2026.1823453

63. Zhou S, He L, Lin W, Su Y, Liu Q, Qu M, Xiao L: **Integrative analysis of transcriptome and metabolism reveals potential roles of carbon fixation and photorespiratory metabolism in response to drought in Shanlan upland rice**. *BMC Genomics* 2022, **23**(1):862. https://doi.org/10.1186/s12864-022-09094-3

Supplementary Files

This is a list of supplementary files associated with this preprint. Click to download.

- Supplementarymaterial.rar